Trajectory Shaping Guidance for Vertical Landing of Launch Vehicle Stage

Dhiraj Kumar Jha,* Athira P V, Gifty Ernestina Benjamin, and Abdul Saleem
Vikram Sarabhai Space Center, Thiruvananthapuram-695022, India

doi: https://doi.org/10.37285/bsp.SACAD2025.24

Abstract- Vertical landing and recovery of rockets have emerged as a critical capability in the development of reusable launch vehicles. This work proposes a trajectory-shaping guidance strategy designed to enable precise and accurate vertical landings. The proposed method defines the downrange position as a function of altitude and employs a linearly decreasing velocity profile to facilitate a smooth and controllable descent. The effectiveness of the guidance strategy is validated through detailed simulation studies, demonstrating its potential for reliable and efficient recovery of launch vehicle stages.

Nomenclature

x, h	= Down-Range, Altitude
v, γ	= Velocity, Flight Path Angle
R_E	= Earth Radius
0	= Subscript for Initial Condition
f	= Subscript for final Condition
T	= Thrust
D	= Drag
I_{sp}	= Specific impulse

I. Introduction

Reusable rocket stages require precise vertical landing capabilities to enable cost-effective and reliable space launch operations. The development of descent guidance algorithms for such vehicles involves addressing highly nonlinear flight dynamics, stringent terminal constraints, and real-time computational requirements. Existing guidance methodologies can be broadly categorized into (i) optimization-based approaches, such as convex optimization, successive convexification, and pseudospectral methods; (ii) feedback-based schemes, including proportional navigation, sliding mode control, and feedback linearization; and (iii) predictive and adaptive strategies, such as model predictive control and adaptive guidance.

Optimization-based methods have received considerable attention due to their ability to handle complex dynamics and constraints with formal guarantees of convergence. Açıkmeşe and Ploen [1] developed a convex programming framework for powered descent guidance, formulating the Mars landing problem as a convex optimization problem that can be solved in real-time with guaranteed global optimality. This pioneering work laid the foundation for subsequent research on real-time trajectory optimization. Building on this, Szmuk and Açıkmeşe [2] extended the
convex framework to full six-degree-of-freedom (6-DOF) dynamics using successive convexification, enabling accurate and computationally efficient solutions for reusable launch vehicle landings under realistic dynamic and operational constraints. In parallel, feedback-based control methods have been developed to provide robustness against modeling errors and external disturbances.

Among these, sliding mode control (SMC), as introduced by Utkin [3], offers strong robustness by driving system states to a sliding surface and maintaining them despite uncertainties. Terminal sliding mode variants further enhance this approach by ensuring finite-time convergence, making them particularly suitable for precise trajectory tracking and rapid stabilization required during the final descent phase of landing. Polynomial guidance schemes offer explicit analytic solutions using low-order thrust or acceleration polynomial profiles. Lu [4] revitalized and extended the Apollo-era “augmented Apollo guidance” algorithms using a quadratic polynomial accelerate on model for precise powered descent. In subsequent work, Lu [5] introduced fractional-polynomial powered descent guidance (FPDG), which encompasses a family of guidance laws including the classical Apollo Lunar Descent Guidance (ALDG) and E-Guidance. The FPDG family permits systematic tuning of algebraic parameters for improved control and constraint handling.

Complementing both optimization and feedback approaches, predictive and adaptive strategies have been investigated to further improve real-time performance and robustness under varying initial conditions and system uncertainties. Jung et al. [6] proposed a model predictive control (MPC) framework combined with sequential convex programming to achieve fuel-optimal landing trajectories, demonstrating accurate performance in 6-DOF simulations with real time feasibility. More recently, Zaragoza Prous et al. [7] introduced a decreasing horizon MPC approach that dynamically adjusts the prediction horizon as the vehicle approaches touchdown, effectively preventing unnecessary hovering and ensuring timely convergence to the terminal landing conditions. These studies collectively illustrate the progressive development of descent guidance algorithms, moving from purely optimization-based formulations to hybrid approaches that integrate feedback, prediction, and adaptation for improved accuracy, robustness, and real-time implementation. This work introduces a trajectory-shaping guidance law that parametrizes downrange position as a function of altitude while imposing a linearly decreasing velocity profile, resulting in smooth descent trajectories capable of satisfying stringent terminal constraints. The paper is structured as follows: Section II outlines the Problem Statement and Dynamical Model, Section III introduces the proposed guidance law, Section IV describes the Mathematical Formulation, Section V presents the simulation results, and the rest of the paper concludes the work.

II. Problem Statement and Dynamical Model

Consider a rocket stage in final phase of vertical landing, the state of the stage is defined in vertical plane with initial state as altitude (h_0), velocity (V_0) and flight path angle (γ_0).

The work aims to develop a guidance law which steers the vehicle from given initial state to the landing site with desired state such as (h_f, V_f, γ_f). The initial and terminal conditions are mentioned in table 1.

	state
Initial condition	h_0, x_0, γ_0, V_0
Final condition	h_f, x_f, γ_f, V_f

Table 1 Boundary Condition for Guidance

The stage is assumed to be a point mass and its motion in vertical plane is defined by following set of ordinary differential equation.

$$\dot{V} = \frac{T\cos\alpha - D}{m} - g\sin\gamma \qquad (1)$$

$$\dot{\gamma} = \frac{T\sin\alpha + L}{mV} - \frac{g\cos\gamma}{V} \qquad (2)$$

$$\dot{h} = V\sin\gamma \qquad (3)$$

$$\dot{x} = V\cos\gamma \qquad (4)$$

$$\dot{m} = \frac{-T}{gI_{SP}} \qquad (5)$$

Where V is the airspeed, T is the thrust magnitude, α is the angle of attack, γ is the flight path angle, g is the Earth's gravitational Acceleration, h is the altitude, x is the down-track position, m is the stage mass, I_{sp} is the specific impulse, D & L is the drag and lift forces as defined in Eq. (6).

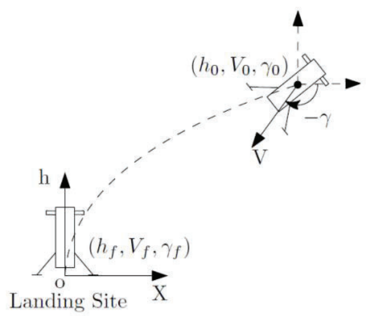

Fig. 1 Terminal Phase of Vertical Landing

$$D = QSC_D,\ L = QSC_L \qquad (6)$$

Where $Q = \frac{1}{2}\rho V^2$

Q is the dynamic pressure, S is the reference area, ρ is the atmospheric density, C_L and C_D are the lift and drag coefficient receptively.

III. Proposed Guidance Law

This section presents the trajectory shaping guidance that shapes the stage trajectory and velocity profile.

A. Trajectory Shaping Guidance

The trajectory of the stage in vertical plane is presented such that downrange is the function of altitude. The trajectory and flight shape is presented as in Eq (8) (9) & (10).

$$x_{ref} = f(h) \qquad (7)$$

$$\frac{dx}{dh} = \cot\gamma \qquad (8)$$

$$x = a_1h^3 + a_2h^2 + a_3h + a_4 \qquad (9)$$

$$\frac{dx}{dh} = 3a_1h^2 + 2a_2h + 3a_3 = \cot\gamma \qquad (10)$$

For a known initial condition (h_0, γ_0) and final condition at landing site (h_f, γ_f), the unknown coefficient of presented guidance can be computed.

$$x_0 = a_1h_0^3 + a_2h_0^2 + a_3h_0 + a_4 \qquad (11)$$

$$x_f = a_1h_f^3 + a_2h_f^2 + a_3h_f + a_4 \qquad (12)$$

$$\left.\frac{dx}{dh}\right|_{h0} = 3a_1h_0^2 + 2a_2h_0 + 3a_3 = \cot\gamma_0 \qquad (13)$$

$$\left.\frac{dx}{dh}\right|_{hf} = 3a_1h_f^2 + 2a_2h_f + 3a_3 = \cot\gamma_f \qquad (14)$$

The equation can be expressed in matrix form Eq. (15),

$$\begin{pmatrix} x_0 \\ x_f \\ \cot\gamma_0 \\ \cot\gamma_f \end{pmatrix} = \begin{bmatrix} h_0^3 & h_0^2 & h_0 & 1 \\ h_f^3 & h_f^2 & h_0 & 1 \\ 3h_0^2 & 2h_0 & 1 & 0 \\ 3h_f^2 & 2h_f & 1 & 0 \end{bmatrix} \begin{bmatrix} a_1 \\ a_2 \\ a_3 \\ a_4 \end{bmatrix} \qquad (15)$$

considering

$$A = \begin{bmatrix} h_0^3 & h_0^2 & h_0 & 1 \\ h_f^3 & h_f^2 & h_0 & 1 \\ 3h_0^2 & 2h_0 & 1 & 0 \\ 3h_f^2 & 2h_f & 1 & 0 \end{bmatrix},\ B = \begin{pmatrix} x_0 \\ x_f \\ \cot\gamma_0 \\ \cot\gamma_f \end{pmatrix}, \text{and } C = \begin{bmatrix} a_1 \\ a_2 \\ a_3 \\ a_4 \end{bmatrix}$$

The vector B contains the boundary condition, the known vector C can be computed by using a inverse of matrix A as described by Eq.(16)

$$C = A^{-1}B \qquad (16)$$

B. Velocity Profile Design

The velocity profile need to be designed to be such that boundary condition mentioned in 1 should be satisfied. As the velocity at 2-points (initial and final state) need to be satisfied, hence a linear velocity profile such as mentioned in (17) can be designed.

$$V = d_1h + d_2 \qquad (17)$$

The equation in matrix form is expressed in (18), the unknown coefficient d_1 and d_2 can be computed using Eq. (19).

$$\begin{bmatrix} V_0 \\ V_f \end{bmatrix} = \begin{bmatrix} h_0 & 1 \\ h_f & 1 \end{bmatrix} \begin{bmatrix} d_1 \\ d_2 \end{bmatrix} \quad (18)$$

considering

$$D = \begin{bmatrix} d_1 \\ d_2 \end{bmatrix}, E = \begin{bmatrix} h_0 & 1 \\ h_f & 1 \end{bmatrix}, \text{and } F = \begin{bmatrix} V_0 \\ V_f \end{bmatrix}$$

$$D = E^{-1} F \quad (19)$$

IV. Mathematical Formulation

This section presents the detailed formulation to compute control forces $F1$, $F2$ and orientation of the vehicle in vertical plane. The equation of motion can be modified such as $F_1 = T\cos\alpha - D,\ F_2 = T\sin\alpha + L.$ Equation (1) & (2) can be re-written as in (20) and (21).

$$\dot{v} = \frac{F_1}{m} - g\sin\gamma \quad (20)$$

$$\dot{\gamma} = \frac{F_2}{mV} - \frac{g\cos\gamma}{V} \quad (21)$$

The control force F_1 and F_2 can be determined such as that design trajectory can be followed. Dividing Eq. (21) with (3) resulted into expression for F_2 in (23).

$$\frac{d\gamma}{dh} = \frac{F_2}{mV_2\sin\gamma} - \frac{g\cos\gamma}{V^2\sin\gamma} \quad (22)$$

$$F_2 = mV^2\sin\gamma\left[\frac{d\gamma}{dh} + \frac{g\cos\gamma}{V^2\sin\gamma}\right] \quad (23)$$

Using Eq.(10),

$$\frac{-1}{\sin^2\gamma}\frac{d\gamma}{dh} = \left(6a_1h + 2a_2\right) \quad (24)$$

$$\frac{d\gamma}{dh} = -\sin^2\gamma\left(6a_1h + 2a_2\right) \quad (25)$$

Similarly dividing Eq. (20) and (3) and rearranging the equation results in Eq. (26),

$$F_1 = mV\sin\gamma\left[\frac{dv}{dh} + \frac{g}{V}\right] \quad (26)$$

Using Eq. (17) and (26),

$$F_1 = mV\sin\gamma\left[d_1 + \frac{g}{v}\right] \quad (27)$$

Eq. (23) and (27) can be re-written as in (28) and (29). The reference angle of attack can be computed by dividing Eq. (28) & (29).

$$T\sin\alpha = mV^2\sin\gamma\left[\frac{d\gamma}{dh} + \frac{g\cos\gamma}{V^2\sin\gamma}\right] - L \quad (28)$$

$$T\cos\alpha = mV\sin\gamma\left[d1 + \frac{g}{V}\right] + D \quad (29)$$

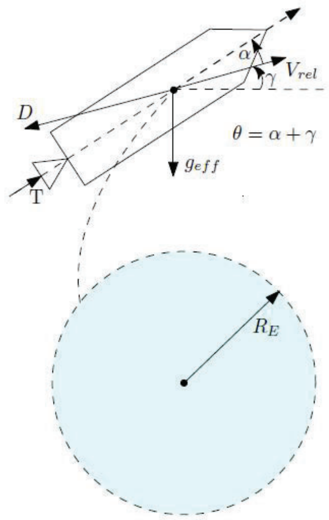

Fig. 2 Definition of Stage Orientation in Vertical Plane

The orientation of the stage and different angles are presented in Fig. 2. Using angle of attack (α) and flight path angle (γ) at an instant, the orientation of stage in vertical plane (θ) can be computed.

V. Simulation Results

This section presents the simulation results that demonstrate the effectiveness of the proposed guidance law.

The performance is evaluated under a nominal scenario, and its robustness is further assessed through Monte Carlo simulations. Given that the thrust force during the terminal phase significantly exceeds the aerodynamic forces, the effects of lift and drag are neglected in the simulation analysis.

	(h, x, γ, V)
Initial condition	$2500m, 3800m, -15°, 200m/s$
Final condition	$0m, 0m, -90°, 0$

Table 2 Boundary Condition for Simulation

A. Nominal Scenario

Considering a nominal scenario for the terminal phase of stage landing, the vehicle begins its descent from an altitude of 2.5, km and a downrange distance of 3.8, km from the landing site, with an initial velocity of 200, m/s. The flight path angle at the onset of the terminal phase is $\gamma = -15\circ$, and the desired flight path angle at touchdown is also $\gamma = -90\circ$. The initial and final conditions for the terminal guidance phase are summarized in Table 2.

Fig. 3a and Fig. 3b illustrate the descent trajectory and the variation of the flight path angle, respectively. The results indicate that both the altitude and flight path angle profiles are smooth and satisfy the specified boundary conditions at landing. Fig. 3c shows the prescribed linearly decreasing velocity profile, while Fig. 3d presents the corresponding thrust profile, which is observed to be continuous and well-behaved throughout the descent phase. Additionally, Fig. 4 shows the variation in steering angle and angle of attack, further validating that the guidance strategy successfully achieves the desired terminal landing conditions.

Fig. 5 presents the time history of the state variables during the terminal phase. It can be observed that the stage reaches an altitude of approximately 50m, indicating that the altitude error reduces to 2% of its initial value within approximately 66s. This duration is defined as the settling time. The figure also demonstrates the convergence of velocity, flight path angle, and downrange distance to their respective desired terminal values, confirming the effectiveness of the proposed guidance strategy in achieving the target landing conditions.

B. Monte-Carlo Simulation

A Monte Carlo simulation is conducted to assess the performance and robustness of the proposed guidance strategy. The initial state variables downrange position ($x0$), velocity ($v0$), and flight path angle ($\gamma 0$) are assumed to follow a uniform distribution. The corresponding maximum and minimum bounds for each variable are summarized in Table 3. A total of 1000 samples are generated for the simulation. The Initiation of the terminal descent phase is sensed based on a fixed altitude threshold the variations in altitude are not considered. This approach enables the evaluation of the guidance law under a range of possible initial conditions, thereby demonstrating its effectiveness in handling variability during the terminal descent phase.

States	$Max.$	$Min.$
Downrange ($x_0 = -3800$m)	$1.1x_0$	$0.9x_0$
Velocity ($v_0 = 200$m/s)	$1.05v_0$	$0.95v_0$
Flight Path Angle ($\gamma_0 = -15°$)	$1.03\gamma_0$	$0.97\gamma_0$

Table 3 Bounds on states for Initial condition perturbation

Figure 6 and Figure 7 depict the trajectory and flight path angle profiles obtained from the Monte Carlo simulation. It can be observed that the guidance law successfully steers the vehicle to the desired terminal state across all perturbed initial conditions. The results align with expectations and demonstrate the effectiveness and robustness of the proposed guidance scheme in handling variations in initial state parameters.

VI. Conclusion

This study presented a trajectory shaping guidance strategy for the vertical landing of reusable launch vehicles, with a focus on achieving precise and smooth terminal descent.

The proposed guidance law was validated through nominal and Monte Carlo simulations, demonstrating its effectiveness in steering the vehicle to the desired terminal state across a range of initial conditions. The simulation results confirm that the guidance scheme ensures smooth profiles for altitude, velocity, flight path angle, and thrust, while satisfying the boundary conditions required for safe landing.

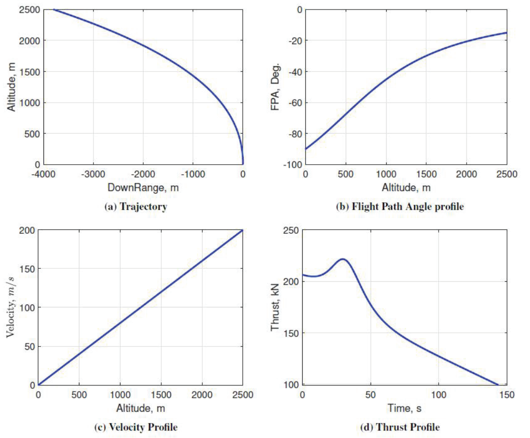

Fig. 3 Simulation Results: Nominal Scenario

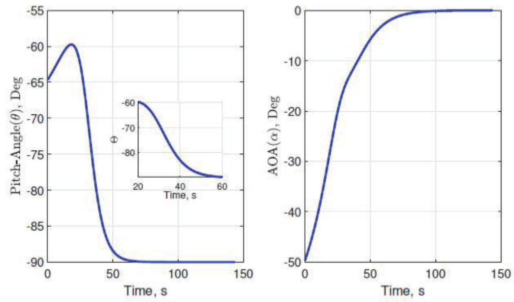

Fig. 4 Simulation Results: steering and angle of Attack Profile

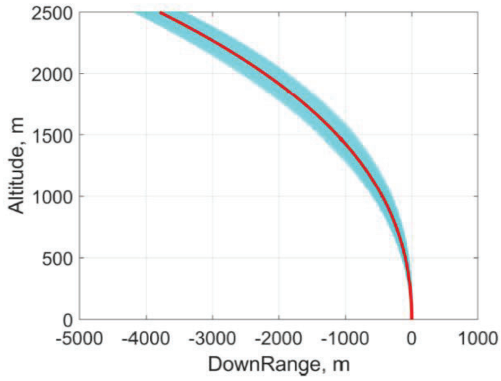

Fig. 6 Simulation Results: trajectory

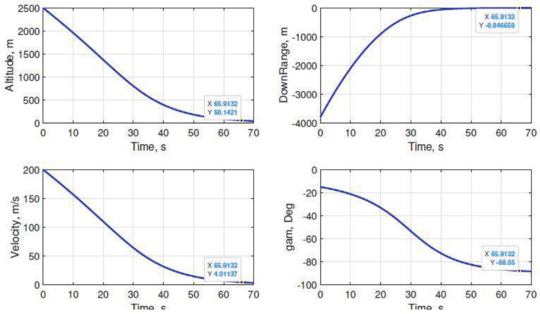

Fig. 5 Simulation Results: Time History of State variable

While the current analysis neglects aerodynamic effects and assumes ideal navigation data, further validation is necessary under more realistic operational scenarios. Future work will focus on evaluating the guidance performance in the presence of atmospheric disturbances such as wind, as well as navigation errors due to sensor noise and biases.

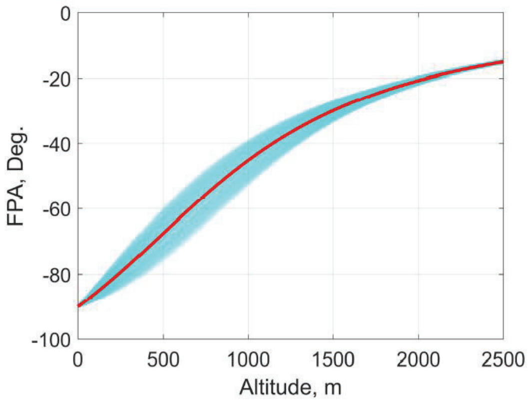

Fig. 7 Simulation Results: Flight Path Angle Profile

Incorporating these factors will be essential to fully assess the robustness and practical viability of the proposed guidance law for real-world applications.

References

1. Açıkmeşe, B., and Ploen, S. R., "Convex Programming Approach to Powered Descent Guidance for Mars Landing," *Journal of Guidance, Control, and Dynamics*, Vol. 30, No. 5, 2007, pp. 1353–1366. https://doi.org/10.2514/1.27553.

2. Szmuk, M., and Açıkmeşe, B., "Successive Convexification for 6-DoF Mars Rocket Powered Landing with Free-Final-Time," *AIAA Guidance, Navigation, and Control Conference*, 2018. https://doi.org/https://doi.org/10.2514/6.2018-0617.

3. Venkataraman, S. T., and Gulati, S., "Control of Nonlinear Systems Using Terminal Sliding Modes," *American Control Conference*, 1992, pp. 1859–1863. https://doi.org/10.23919/ACC.1992.4792209.

4. Lu, P., "Augmented Apollo Powered Descent Guidance," *Journal of Guidance, Control, and Dynamics*, Vol. 42, No. 3, 2019, pp.447–457. https://doi.org/10.2514/1.g004048.

5. Lu, P., "Theory of Fractional-Polynomial Powered Descent Guidance," *Journal of Guidance, Control, and Dynamics*, Vol. 43, No. 3, 2020, pp. 398–409. https://doi.org/10.2514/1.g004556.

6. Jung, K.-W., Lee, S.-D., Jung, C.-G., and Lee, C.-H., "Model Predictive Guidance for Fuel-Optimal Landing of Reusable Launch Vehicles," *Aerospace Science and Technology*, Vol. 143, 2024, p. 108017. https://doi.org/10.48550/arXiv.2405.01264.

7. Zaragoza Prous, G., Grustan-Gutierrez, E., and Felicetti, L., "A Decreasing Horizon Model Predictive Control for Landing Reusable Launch Vehicles," *Aerospace*, Vol. 12, No. 2, 2025, p. 111. https://doi.org/10.3390/aerospace12020111.